

# PROBE FOR TYPE IA SUPERNOVA PROGENITOR IN DECIHERTZ GRAVITATIONAL WAVE ASTRONOMY

TOMOYA KINUGAWA

Department of Astronomy, University of Tokyo, Bunkyo, Tokyo 113-0033, Japan

HIROKI TAKEDA

Department of Physics, University of Tokyo, Bunkyo, Tokyo 113-0033, Japan

HIROYA YAMAGUCHI

Institute of Space and Astronautical Science, JAXA, 3-1-1 Yoshinodai, Sagamihara, Kanagawa 229-8510, Japan and  
Department of Physics, University of Tokyo, Bunkyo, Tokyo 113-0033, Japan

(Dated: January 25, 2022)  
*Draft version January 25, 2022*

## ABSTRACT

It is generally believed that Type Ia supernovae are thermonuclear explosions of carbon-oxygen white dwarfs (WDs). However, there is currently no consensus regarding the events leading to the explosion. A binary WD (WD-WD) merger is a possible progenitor of Type Ia supernovae. Space-based gravitational wave (GW) detectors with great sensitivity in the decihertz range like DECIGO can observe WD-WD mergers directly. Therefore, access to the deci-Hz band of GWs would enable multi-messenger observations of Type Ia supernovae to constrain their progenitor and explosion mechanism. In this paper, we consider the event rate of WD-WD mergers and minimum detection range to observe one WD-WD merger per year, using nearby galaxy catalog and the relation between the Ia supernova and the host galaxy. Furthermore, we calculate the DECIGO's ability to localize WD-WD mergers and to determine the masses of binary mergers. We estimate that if the deci-Hz GW observatory can detect the GW whose amplitude is  $h \sim 10^{-20}[\text{Hz}^{-1/2}]$  at 0.1 Hz, 1000 times higher than the detection limit of DECIGO. In fact, DECIGO is expected to detect WD-WD ( $1M_{\odot} - 1M_{\odot}$ ) mergers within  $z = 0.115$ , corresponding to the detection rate of  $\sim 20000 \text{ yr}^{-1}$ , and identify the host galaxy of WD-WD mergers for  $\sim 8000$  WD-WDs only by the GW detection.

## 1. INTRODUCTION

Advanced LIGO have detected GWs from compact binary mergers. These results reveal the existence of massive stellar black holes, and the origin of the r-process elements and short gamma-ray burst (Abbott et al. 2016a,b, 2017). Now we are in the dawn of GW astronomy. Ground GW detectors such as advanced LIGO, advanced VIRGO, and KAGRA cover 10-10,000 Hz. LISA is planned to detect the milli Hz GW and will launch at 2030s (Amaro-Seoane et al. 2017). DECIGO and B-DECIGO, a test version of DECIGO, fill the gap between the ground GW detectors and LISA (Seto et al. 2001; Nakamura et al. 2016). The main target of DECIGO is the stochastic background GW from the early universe. Design sensitivity of DECIGO and B-DECIGO are  $h \sim 10^{-23}-10^{-24}[\text{Hz}^{-1/2}]$ , and  $h \sim 10^{-22}-10^{-23}[\text{Hz}^{-1/2}]$  at 0.1-10 Hz, respectively. These sensitivities are very useful to detect high redshift binary black hole mergers and check the origin of massive stellar binary black holes (e.g. Kinugawa et al. 2014; Kinugawa et al. 2016; Belczynski et al. 2016; Nakamura et al. 2016). Furthermore, the GW from a WD-WD merger is also  $\sim 0.1$  Hz (Mandel et al. 2018). Thus, WD-WD mergers will become interesting science targets of DECIGO (Seto et al. 2001; Mandel et al. 2018) and other 0.1Hz GW

detectors such as B-DECIGO (Nakamura et al. 2016), TianGO (Kuns et al. 2019), DO(Arca Sedda et al. 2019) and AMIGO (Ni et al. 2019).

WD-WD mergers are one of the most promising candidates of Ia supernova progenitors. Despite the important use of Ia supernovae as distance indicators in cosmology, many fundamental aspects of their evolution and explosion are still under debate. There are two competing hypotheses for the Ia supernova progenitor system. One is the single degenerate (SD) scenario, where a close binary system consisting of a C-O WD and a non-degenerate companion, such as a main-sequence star or red giant, are considered (Whelan, & Iben 1973). The WD explodes when its mass grows close to the Chandrasekhar limit ( $\sim 1.4M_{\odot}$ ) via mass transfer from the companion (e.g. Nomoto 1982; Hachisu et al. 1996). The other is the double degenerate (DD) scenario, which assumes a dynamical merger or disruption of two WDs as the origin of the explosion. The DD models can be further subdivided into the classical DD (e.g. Webbink 1984; Iben, & Tutukov 1984), violent merger (e.g. Pakmor et al. 2010; Sato et al. 2015), and dynamically-driven double-degenerate double-detonation ( $D^6$ ) scenarios (e.g. Woosley, & Kasen 2011; Shen, & Bildsten 2014). The classical DD model assumes the fast accretion ( $\sim 10^{-5}M_{\odot} \text{ yr}^{-1}$ ) of the disrupted secondary (lighter WD) onto the surface of the primary (more massive WD). The primary WD explodes when the C-O core mass gets close to the Chandrasekhar limit, similarly to the consequence of the SD scenario,

unless it collapses to a neutron star. The other two scenarios assume a much shorter timescale ( $\lesssim 100$  s) of the merging process and a sub-Chandrasekhar-mass explosion of the primary. An important difference between the two models is that the secondary also explodes in the former but remains intact in the latter. Notably, the relation between the primary WD mass and the synthesized  $^{56}\text{Ni}$  mass (hence peak brightness) significantly differs between the two models. For instance, a light curve of normal brightness Ia supernovae is well reproduced by a primary mass of  $1.1M_{\odot}$  in the violent merger (Pakmor et al. 2012) whereas  $1.0M_{\odot}$  in the  $D^6$  explosion (Shen et al. 2018). As we demonstrate later, GW observations will determine the accurate mass of WDs in the binary system, constraining the progenitor and explosion mechanism of Ia supernovae with coordinated observations in the optical wavelength, i.e., multi-messenger astronomy.

In this letter, we consider the event rate of WD-WD mergers and minimum detection range to observe one WD-WD merger per year, using nearby galaxy catalog and the relation between the Ia supernova and the host galaxy (§1). Furthermore, we calculate DECIGO’s detection rate and ability to localize WD-WD mergers and to determine the masses of binary mergers (§3, 4.2, and 5). Throughout this paper we use CGS units.

## 2. EVENT RATE OF WD-WD MERGERS

Badenes, & Maoz (2012) shows that the local Ia supernova rate per unit stellar mass in our galaxy is consistent with the WD-WD merger rate per unit stellar mass including sub-Chandrasekhar WD-WD merger cases. In order to estimate the WD-WD merger rate, we assume that all the Ia supernova progenitors are the WD-WD mergers. The Ia supernova rate at  $z \sim 0$  is

$$(0.301 \pm 0.062) \times 10^{-4} \text{SN yr}^{-1} \text{Mpc}^{-3}, \quad (1)$$

determined from the Lick Observatory Supernova Search (LOSS) (Li et al. 2011). We use this value as the fiducial rate of WD-WD mergers to estimate the detection rate in this paper. However, this rate is the averaged volumetric rate of Ia supernova. There are many studies of the correlation between the Ia supernova rate and the host galaxy property (e.g. Sullivan et al. 2006; Totani et al. 2008; Li et al. 2011; Graur et al. 2015) and these results indicate the relation between Ia supernova rate and the stellar mass of the galaxies. In order to estimate how much sensitivity can detect one Ia supernova per year, we estimate the Ia supernova rate at nearby galaxies using the rate-size relation of Ia supernova host galaxy (Li et al. 2011) and the catalog of nearby galaxies within 11 Mpc (Karachentsev et al. 2013). The rate-size relation is

$$\text{SNuM} = \text{SNuM}(M_0) \times \left( \frac{M_*}{10^{10}M_{\odot}} \right)^{\text{RSS}}, \quad (2)$$

where SNuM, SNuM( $M_0$ ),  $M_*$ , and RSS are the Ia supernova rate per century per  $10^{10}M_{\odot}$ , the normalization value, the stellar mass of the galaxy, and the power law index, respectively. Li et al. (2011) obtained  $-0.513 \pm 0.316$ ,  $-0.503 \pm 0.158$ ,  $-0.637 \pm 0.199$ ,  $-0.555 \pm 0.171$ ,  $-0.443 \pm 0.241$ ,  $-0.329 \pm 0.201$ , and  $-0.435 \pm 0.195$  as RSSs for E, S0, Sa, Sb, Sbc, Sc, and Scd galaxies. These values are around -0.5, so we adopt

0.50 and 0.25 as RSS and SNuM( $M_0$ ) in our rate calculations, respectively. The combined significance with RSS=-0.5 and SNuM( $M_0$ )=0.25 for E, S0, Sa, Sb, Sbc, Sc, and Scd galaxies is  $7.4\sigma$  (Li et al. 2011).

We use the galaxy catalog of Karachentsev et al. (2013) in order to get the stellar mass of nearby galaxies. In this catalog, there are 1209 galaxies data within 11 Mpc and 951 galaxies’ masses or lower mass limits are known. Figure 1 shows the stellar mass distribution of nearby galaxies. In the case of galaxies whose masses  $\lesssim 10^5 M_{\odot}$  in Fig. 1, we use lower mass limits of galaxies as galaxy stellar masses.

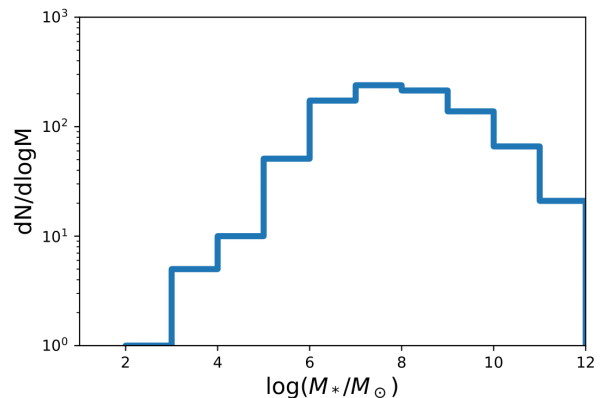


FIG. 1.— The stellar mass distribution of nearby galaxies within 11 Mpc.

We combine the equation 2 and masses in this catalog data and calculate the Ia supernova rate in nearby galaxies within 11 Mpc. The Ia supernova rate in nearby galaxies is

$$0.85 \text{ yr}^{-1}. \quad (3)$$

Thus, if the detection range of GW detector on  $\sim 0.1$ Hz band is 11Mpc, we can observe about one Ia supernova per year and check whether Ia supernova progenitors are WD-WD mergers or not.

## 3. GRAVITATIONAL WAVE OBSERVATIONS FROM BINARY SYSTEM WITH SPACE-BASED DETECTOR

In general relativity, the detector signal of inspiral GWs from binary coalescence in time domain can be expressed as below (Berti et al. 2005),

$$h(t) \simeq \frac{2m_1m_2}{r_s(t)D_L} \mathcal{A}(t) \cos \left( \int^t f_{\text{gw}}(t') dt' + \phi_p(t) + \phi_D(t) \right), \quad (4)$$

where  $m_1, m_2$  are the masses of binary stars,  $r_s(t)$  is the orbital relative distance,  $D_L$  is the luminosity distance to the binary system,  $f_{\text{gw}}$  is the frequency of the GW, and  $\phi_D(t)$  is the doppler phase.  $\mathcal{A}(t)$  and  $\phi_p(t)$  are defined by,

$$\mathcal{A}(t) := \sqrt{(1 + \cos^2 \iota)^2 F^+(t)^2 + 4 \cos^2 \iota F^\times(t)^2}, \quad (5)$$

$$\phi_p(t) := \arctan \left( \frac{2 \cos \iota F^\times(t)}{(1 + \cos^2 \iota) F^+(t)} \right). \quad (6)$$

where  $\iota$  is the inclination angle of the binary system,  $F^+$  and  $F^\times$  are the antenna pattern functions for the plus

and cross mode of the GW, respectively.

The Fourier components  $h(f)$  of the detector signal  $h(t)$  can be derived by the stationary phase approximation, since  $(2m_1m_2)/(r_s(t)D_L)$ ,  $\mathcal{A}(t)$ ,  $\phi_p$ ,  $\phi_D$  vary in time slowly compared to  $\int f_{\text{gw}}(t')dt'$ . Employing stationary phase approximation, we obtain the Fourier components of the detector signal (Maggiore 2007; Berti et al. 2005; Cutler 1998; Arun 2006),

$$h_I(f) = \mathcal{A}f^{-7/6}e^{i\Psi(f)} \left\{ \frac{5}{4}\mathcal{A}(t(f)) \right\} e^{-i(\phi_p(t(f))+\phi_D(t(f)))}. \quad (7)$$

The geometrical factor for tensor modes  $\mathcal{G}_{T,I}$  is defined by

$$\mathcal{G}_{T,I} := \frac{5}{4}\{(1 + \cos^2 \iota)F_{+,I}(t) + 2i \cos \iota F_{\times,I}(t)\}e^{i\phi_{D,I}(\theta_s, \phi_s, \theta_e, \phi_e)}, \quad (8)$$

where  $(\theta_s, \phi_s)$  and  $(\theta_e, \phi_e)$  are the angular parameters denoting the source direction and the detector position, respectively. The geometrical factor is normalized by the factor of 5/4 such that the average of Eq. (8) over angular parameters gives unity. Finally we get the Fourier components  $h(f)$  with the amplitude,  $\mathcal{A}$  and the phase,  $\Psi(f)$ ,

$$h_I(f) = \mathcal{A}f^{-7/6}e^{i\Psi(f)}\mathcal{G}_{T,I}(t(f)). \quad (9)$$

$t(f)$  is defined by the condition  $f = f_{\text{gw}}(t(f))$ ,

$$t(f) := t_c - \frac{5}{256}\mathcal{M}^{-5/3}(\pi f)^{-8/3}, \quad (10)$$

where  $\mathcal{M} := (m_1m_2)^{3/5}(m_1 + m_2)^{-1/5}$  is the chirp mass and  $t_c$  is the coalescence time. For equal mass binary whose total mass is  $M_{\text{tot}}$ ,  $\mathcal{M} = 4^{-3/5}M_{\text{tot}} \sim 0.435M_{\text{tot}}$ . Thus, it gives the relation between the time to coalescence and the frequency of the GW before merger.

## 4. PARAMETER ESTIMATION

### 4.1. Waveform

We adopt the inspiral waveform up to Newtonian order in amplitude  $\mathcal{A}$  and 3.5 post-Newtonian (PN) order in phase  $\Psi(f)$  (Khan et al. 2016),

$$h_{\text{GR}} = \mathcal{A}f^{-7/6}e^{i\Psi(f)}, \quad (11)$$

with

$$\mathcal{A}f^{-7/6} = \frac{1}{\sqrt{30}\pi^{2/3}d_L}\mathcal{M}^{5/6}f^{-7/6}, \quad (12)$$

and

$$\Psi(f) = 2\pi ft_c - \phi_c - \frac{\pi}{4} + \frac{3}{128}(\pi\mathcal{M}f)^{-5/3} \sum_{i=0}^7 \phi_i(\pi\mathcal{M}f)^{i/3}. \quad (13)$$

The amplitude part of the waveform is kept up to the Newtonian order because we consistently deal with the waveform at the same order as the expression in Eq. (10). WD-WDs are expected to have circular orbits due to tidal interactions (Willems et al. 2007; Ruiter et al. 2010). It was reported that the deformations due to filling the Roche lobe or the existence accretion disk induce typical difference at the level of one percent or less for semi-detached WD-WDs with respect to the average

strain amplitude (van den Broek et al. 2012). We use the above inspiral waveform and the point mass approximation without the tidal deformation effect for the sake of clarity.

Therefore, we have 11 model parameters in GR

$$(\log \mathcal{M}, \log \eta, t_c, \phi_c, \log d_L, \chi_s, \chi_a, \theta_s, \phi_s, \cos \iota, \psi_p), \quad (14)$$

where  $\log \eta, \chi_s, \chi_a$  are the logarithm of the symmetric mass ratio  $\eta := m_1m_2/(m_1 + m_2)^2$ , the symmetric and the antisymmetric spin parameter, respectively. We assume that the fiducial values of  $t_c, \phi_c, \chi_s, \chi_a$  are zero. The priors are imposed for parameters having domain of definition;  $\log \eta, \phi_c$ , angular parameters  $(\theta_s, \phi_s, \cos \iota, \psi_p)$ , and binary spin parameters  $(\chi_s, \chi_a)$ .

### 4.2. Analysis and setup

We conducted the model parameter estimation by a Fisher information matrix (Finn 1992; Cutler, & Flanagan 1994). A Fisher information matrix gives the the Cramer-Rao bound of the system parameter and the correlation coefficients between two parameters. In other words, a Fisher information matrix tells us how precisely we can determine the model parameters by observations and how strongly the model parameters are correlated under strong signal and Gaussian noise assumptions. The Fisher information matrix  $\Gamma$  is calculated by

$$\Gamma_{ij} := 4\text{Re} \int_{f_{\text{min}}}^{f_{\text{max}}} df \sum_I \frac{1}{S_{n,I}(f)} \frac{\partial h_I^*(f)}{\partial \lambda^i} \frac{\partial h_I(f)}{\partial \lambda^j}, \quad (15)$$

where  $S_{n,I}(f)$  is the I-th detector noise power spectrum and  $\lambda^i$  is the i-th model parameter. The inverse of the Fisher information matrix gives the root mean square error of a parameter. The root mean square error of  $\Delta\lambda^i$  is calculated by,

$$(\Delta\lambda^i)_{\text{rms}} := \sqrt{\langle \Delta\lambda^i \Delta\lambda^i \rangle} = \sqrt{(\Gamma^{-1})^{ii}}, \quad (16)$$

where  $\Delta\lambda^i$  is the measurement error of  $\lambda^i$  and  $\langle \cdot \rangle$  stands for ensemble average.

The sky localization error is defined by

$$\Delta\Omega_s := 2\pi |\sin \theta_s| \sqrt{\langle (\Delta\theta_s)^2 \rangle \langle (\Delta\phi_s)^2 \rangle - \langle \Delta\theta_s \Delta\phi_s \rangle^2}. \quad (17)$$

Hereafter, we simply refer to  $(\Delta\lambda_i)_{\text{rms}}$  as  $\Delta\lambda_i$ , and call it the estimation error of  $\lambda_i$ .

We conducted Fisher analysis with DECIGO on behalf of decihertz gravitational wave detectors. We assume that DECIGO has its design sensitivity and its orbit is heliocentric orbit.

### 4.3. Cutoff frequency for white dwarf binary

The frequency of the GW from a white dwarf binary at coalescence time can be estimated by the radius and the masses of the stars as follows. We consider a binary system formed by two stars with masses  $m_1$  and  $m_2$ , positions  $\mathbf{r}_1$  and  $\mathbf{r}_2$ , and radius  $R_1$  and  $R_2$ . The dynamics reduces to a one-body problem with mass equal to reduced mass  $\mu = m_1m_2/(m_1 + m_2)$  and EoM  $\ddot{r} = -(GM_{\text{tot}}/r^3)r$  in the center-of-mass frame within Newton approximation. Here,  $r = r_2 - r_1$  is the relative coordinate. Thus, the orbital frequency  $\omega_s$  is related to the orbital radius  $R$  by Kepler's law,

$$\omega_s^2 = \frac{GM_{\text{tot}}}{R^3}, \quad (18)$$

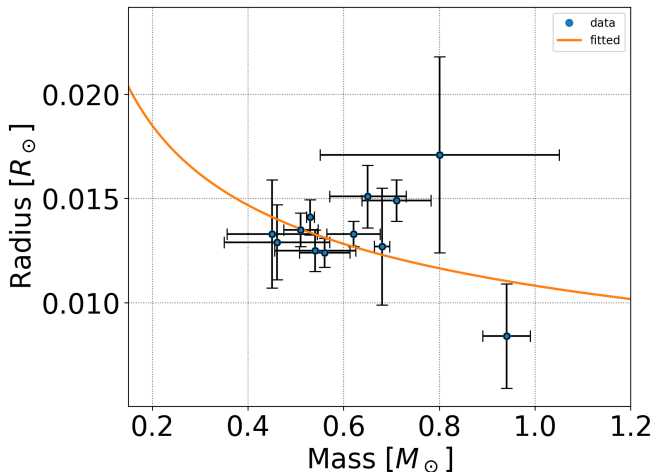


FIG. 2.— Fitting in mass-radius relation for white dwarf star. The data is based on the figure 1. in Magano(2017).

for circular orbits. When the binary stars coalesce, the orbital frequency at that time  $\omega_{s0}$  could be estimated by the following equation,

$$\omega_{s0}^2 = \frac{GM_{\text{tot}}}{(R_1 + R_2)^3}. \quad (19)$$

The frequency of the GW emitted from a binary system is twice the orbital frequency. Therefore, we set the the upper cutoff frequency end  $f_{\text{max}}$  to the frequency, then it is given by

$$f_{\text{max}} \simeq \frac{\omega_s}{\pi} = \frac{1}{\pi} \sqrt{\frac{GM_{\text{tot}}}{(R_1 + R_2)^3}}. \quad (20)$$

In equilibrium, the gravitational pressure should be balanced by the electron pressure. The mass radius relation for WDs is given by the equilibrium condition(Koester & Chanmugam 1990),

$$R_* \propto \frac{\pi m^4 c^5}{3h^3 G(\rho_0 \mu_e)^{5/3}} M_*^{-1/3}, \quad (21)$$

where  $R_*$ ,  $M_*$ ,  $m$ ,  $\mu_e$  are the radius, the mass of a WD, the electron mass, and molecular weight per electron, respectively. Here  $\rho_0 = nH/(p_F/mc)^3$  is a constant where  $n$  is the electron number of density,  $H$  is the atomic mass unit, and  $p_F$  is the Fermi momentum. The radius of a WD is inversely proportional to the cube root of its mass. Figure 2 shows the result of fitting based on the observational data of the mass and radius for white dwarf stars from (Magano et al. 2017). Finally, we adopt the following mass-radius relation for calculation of the upper cutoff frequency.

$$R_* \sim 0.011 \left( \frac{M_*}{M_\odot} \right)^{-1/3} R_\odot \quad (22)$$

Once the upper cutoff frequency is determined, the lower cutoff frequency is determined by the integration time or the observational time through Eq. (10).

## 5. RESULTS

### 5.1. Full 3 year observation

Here, we consider full observation during 3 year operation period and the lower cutoff frequency  $f_{\text{min}}$  is set by the period and the frequency of the GW at the coalescence time.

Table 1 shows the results of Fisher analysis. We estimated parameters for 500 binary system whose angular parameters are uniformly random. The binary masses and the redshift are fixed for the 500 binary system such that the median value of SNR becomes 8, in order to investigate the detectable range with the different fixed mass;  $1M_\odot - 1M_\odot$ ,  $0.8M_\odot - 0.8M_\odot$ , and  $0.6M_\odot - 0.6M_\odot$ . The median values of SNR and errors of the luminosity distance, the sky localization, and the chirp mass are shown.

The median value of SNR is approximately equal to 8 when  $z = 0.115 \sim 550$  Mpc for  $1M_\odot - 1M_\odot$  WD-WD,  $z = 0.049 \sim 224$  Mpc for  $0.8M_\odot - 0.8M_\odot$  WD-WD, and  $z = 0.016 \sim 71$  Mpc for  $0.6M_\odot - 0.6M_\odot$  WD-WD. Thus, the detectable volume can be estimated as  $6.97 \times 10^8 \text{ Mpc}^3$ ,  $4.71 \times 10^7 \text{ Mpc}^3$ , and  $1.50 \times 10^6 \text{ Mpc}^3$ , respectively. Using Eq. (1), it is expected that about 50-2000 Ia supernovae would occur per year during the observational period within the range. Therefore, we will be able to probe for Type Ia supernova progenitors from observations of both gravitational waves and Type Ia supernovae. From Table 1, the 3D localization volumes are estimated by  $513 \text{ Mpc}^3$ ,  $58.3 \text{ Mpc}^3$ , and  $3.92 \text{ Mpc}^3$ , for  $1M_\odot$ ,  $0.8M_\odot$ , and  $0.6M_\odot$  equal mass binary, respectively.

Inversely, ten events are expected per year within  $z = 0.00968$  that is 43 Mpc. Table 2 shows the parameter estimation result in the case of  $z=0.00968$  for  $1M_\odot - 1M_\odot$  WD-WD. The 3D localization volume is estimated as  $7.37 \times 10^{-5} \text{ Mpc}^3$ .

### 5.2. For multi-messenger observation

We studied how the determination accuracy change with the different observation time for multi-messenger observation. For  $1M_\odot$  equal mass WD binary, 1 year, 1 month, 1 week and 1 day before merger correspond to the frequency of the radiated GW, 0.08399, 0.08558, 0.08570 and 0.08573 Hz, respectively. The GWs emitted from WD-WDs are regarded as almost monochromatic waves. The SNR is increasing as  $\text{SNR}^2 \sim h_{\text{amp}} T / S_n(f)$ . Therefore, the errors can be estimated as functions of the observational time for WD-WDs at  $z = 0.00968$  because they are scaled by the SNR as far as the degeneracy among parameters is broken,

$$\Delta \ln d_L \sim 2.29 \times 10^{-2} \times \left( \frac{T}{3 \text{ year}} \right)^{-1/2}, \quad (23)$$

$$\Delta \Omega_s \sim 1.33 \times 10^{-4} \times \left( \frac{T}{3 \text{ year}} \right)^{-1}, \quad (24)$$

$$\Delta \ln \mathcal{M} \sim 1.29 \times 10^{-8} \times \left( \frac{T}{3 \text{ year}} \right)^{-1/2}. \quad (25)$$

Figure 3 shows the dependence of the expected errors on the observational time.

Thus, even one year before merge, which is corresponding to two-year observation, the localization at the level of  $\sim 1.36 \times 10^{-4} \text{ Mpc}^3$  is expected.

TABLE 1  
 MEDIANS OF PARAMETER ESTIMATION ERRORS FOR WD BINARY HAVING DIFFERENT MASSES AND FIXED REDSHIFT AT WHICH THE MEDIAN VALUE OF THE SNR IS EQUAL TO 8. THE REDSHIFT GIVES THE DETECTION RANGE.

parameter	WD-WD( $1M_{\odot}$ , $z=0.115$ )	WD( $0.8M_{\odot}$ , $z=0.049$ )	WD( $0.6M_{\odot}$ , $z=0.016$ )
SNR	8.14	8.12	8.02
$\Delta \ln d_L$	$3.25 \times 10^{-1}$	$3.80 \times 10^{-1}$	$5.11 \times 10^{-1}$
$\Delta \Omega_s [\text{deg}^2]$	$3.11 \times 10^{-2}$	$4.47 \times 10^{-2}$	$7.02 \times 10^{-2}$
$\Delta \ln \mathcal{M}$	$1.83 \times 10^{-7}$	$1.03 \times 10^{-7}$	$7.91 \times 10^{-8}$

TABLE 2  
 MEDIANS OF PARAMETER ESTIMATION ERRORS FOR WD BINARY AT 43 Mpc SO THAT ABOUT TEN TYPE IA SUPERNOVAE ARE EXPECTED WITHIN THE RANGE.

parameter	WD-WD( $1M_{\odot}$ , $z=0.00968$ )
SNR	114
$\Delta \ln d_L$	$2.29 \times 10^{-2}$
$\Delta \Omega_s [\text{deg}^2]$	$1.33 \times 10^{-4}$
$\Delta \ln \mathcal{M}$	$1.29 \times 10^{-8}$

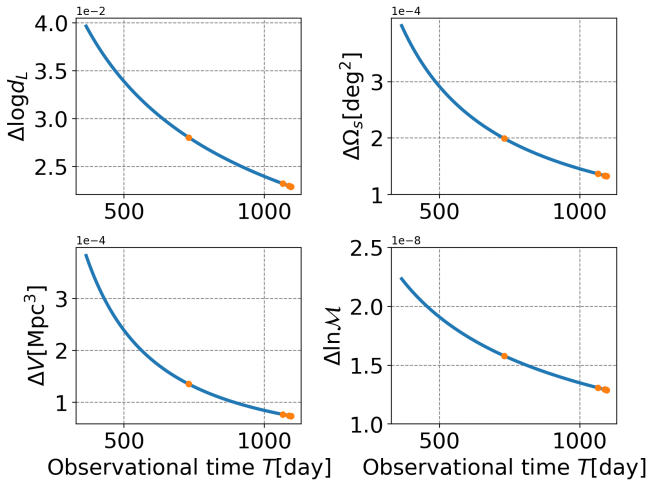


FIG. 3.— The estimation errors vs the observational time for  $1M_{\odot} - 1M_{\odot}$  WD-WD binary at  $z = 0.00968$ . The orange dots show 1 year, 1 month, 1 week and 1 day before merger.

## 6. DISCUSSION & CONCLUSIONS

If the detection range of the deci-Hz detector is  $D_L \sim 11\text{Mpc}$ , we may observe one WD-WD merger event per year. We need  $h < 10^{-20} [\text{Hz}^{-1/2}]$  as the detection sensitivity around 0.1 Hz. In Fig. 4, the AMIGO's sensitivity is same as this value, so the SNR may be small  $\sim 1-2$ . On the other hand, the sensitivities of TianGO and B-DECIGO are  $\sim 3 \times 10^{-22} [\text{Hz}^{-1/2}]$ . DO's sensitivity is  $\sim 5 \times 10^{-23} [\text{Hz}^{-1/2}]$ . Thus, TianGO, B-DECIGO, and DO are sensitive enough to detect a WD-WD merger whose SNR is more than 8.

In the case of a  $1M_{\odot} - 1M_{\odot}$  WD binary, DECIGO can detect its merger event within  $z = 0.115$ , corresponding to the detection rate of  $\sim 20000 \text{ yr}^{-1}$ . Furthermore, DECIGO can detect many inspirals of WD-WDs more than 3 years before their merger at the 0.01-0.1 Hz range. Thus, we can investigate the mass and separation distribution of the WD binaries and the relation between them and their host galaxies. Note that the detection rate esti-

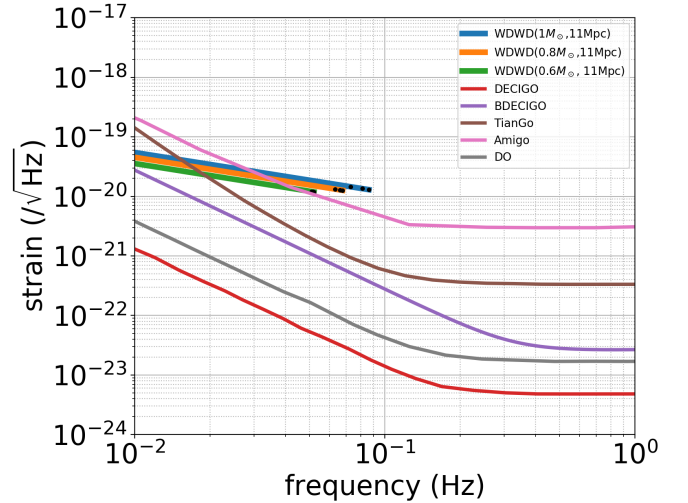


FIG. 4.— The sensitivities of deci-Hz detectors and WD-WD inspirals with different mass. The upper cutoff frequency is determined by Eq. (20). The black points correspond to 10 year, 3 year before merger, and the upper cutoff frequency.

mate strongly depends on masses of WDs, since the GW frequency is proportional to the total mass of WD-WD (Eqs. 20 and 21). If the typical mass of WD-WD mergers is  $0.6M_{\odot} - 0.6M_{\odot}$ , the detection rate lowers down to  $55 \text{ yr}^{-1}$ .

Since the uncertainty in the chirp mass estimate is  $\Delta \ln \mathcal{M} \lesssim 10^{-7}$ , we can easily distinguish the near- and sub-Chandrasekhar-mass explosions. Moreover, since the relation between the primary WD mass and optical luminosity of Ia supernovae depends on the explosion mechanisms (see §1), combination of GW and electromagnetic observations will further distinguish the subclasses of the sub-Chandrasekhar-mass scenarios, i.e., violent merger (e.g., Pakmor et al. 2012) and  $D^6$  (e.g., Shen et al. 2018). It should also be noted that the gravitational signal of the merger phase itself might be different between the two sub-Chandrasekhar scenarios because of the consequence (exploding or remaining) of the secondary WD. In our subsequent paper (Takeda et al. in prep.), we will comprehensively investigate the GW signals for WD-WD mergers with different explosion mechanisms and different WD mass, including non-equal mass binary cases.

The 3D localization volume of DECIGO for  $1M_{\odot} - 1M_{\odot}$  WD-WD mergers at  $z = 0.115$  is  $513 \text{ Mpc}^3$ . This value is proportional to  $d_L^{-6}$ . Thus, the 3D localization volume for  $\sim 8000$  WD-WD mergers within  $d_L \sim 400 \text{ Mpc}$  ( $z = 0.12$ ) is  $\sim 100 \text{ Mpc}^3$ . The galaxy density is one galaxy per  $100 \text{ Mpc}^3$  (Kopparapu et al. 2008), so we can identify host galaxies for many WD-

WD mergers only by the GW detection. Therefore, we can check what astrophysical phenomena occur at the galaxy even if the WD-WD merger does not accompany a Ia supernova.

#### ACKNOWLEDGEMENTS

Thank Makoto G. Ando, Takashi Nakamura, Atsushi Nishizawa, Masaki Ando, Koshiro Shimasaku,

Naoki Seto, Takayuki Sudoh for useful discussion. This work was supported by JSPS KAKENHI Grant No. 18J00558(TK), 18J21016(HT), and 19H00704(HY). HT acknowledge financial support received from the Advanced Leading Graduate Course for Photon Science (ALPS) program at the University of Tokyo.

#### REFERENCES

- Abbott, B. P., Abbott, R., Abbott, T. D., et al. 2016a, *Physical Review Letters*, 116, 061102
- Abbott, B. P., Abbott, R., Abbott, T. D., et al. 2016b, *ApJL*, 818, L22
- Abbott, B. P., Abbott, R., Abbott, T. D., et al. 2017, *Phys. Rev. Lett.*, 119, 161101
- Amaro-Seoane, P., Audley, H., Babak, S., et al. 2017, arXiv e-prints, arXiv:1702.00786
- Arca Sedda, M., Berry, C., Jani, K., et al. 2019, arXiv e-prints, arXiv:1908.11375
- Arun, K. G. 2006, *Phys. Rev. D*, 74, 024025
- Badenes, C., & Maoz, D. 2012, *ApJ*, 749, L11
- Belczynski, K., Holz, D. E., Bulik, T., et al. 2016, *Nature*, 534, 512
- Berti, E., Buonanno, A., & Will, C. M. 2005, *Phys. Rev. D*, 71, 084025
- Cutler, C., & Flanagan, É. E. 1994, *Phys. Rev. D*, 49, 2658
- Cutler, C. 1998, *Phys. Rev. D*, 57, 7089
- Finn, L. S. 1992, *Phys. Rev. D*, 46, 5236
- Graur, O., Bianco, F. B., & Modjaz, M. 2015, *MNRAS*, 450, 905
- Hachisu, I., Kato, M., & Nomoto, K. 1996, *ApJ*, 470, L97
- Iben, I., & Tutukov, A. V. 1984, *ApJS*, 54, 335
- Karachentsev, I. D., Makarov, D. I., & Kaisina, E. I. 2013, *AJ*, 145, 101
- Koester, D., & Chanmugam, G. 1990, *Reports on Progress in Physics*, 53, 837
- Khan, S., Husa, S., Hannam, M., et al. 2016, *Phys. Rev. D*, 93, 044007
- Kinugawa, T., Inayoshi, K., Hotokezaka, K., Nakauchi, D., & Nakamura, T. 2014, *MNRAS*, 442, 2963
- Kinugawa, T., Miyamoto, A., Kanda, N., & Nakamura, T. 2016, *MNRAS*, 456, 1093
- Kopparapu, R. K., Hanna, C., Kalogera, V., et al. 2008, *ApJ*, 675, 1459
- Kuns, K. A., Yu, H., Chen, Y., et al. 2019, arXiv e-prints, arXiv:1908.06004
- Li, W., Chornock, R., Leaman, J., et al. 2011, *MNRAS*, 412, 1473
- Magano, D. M. N., Vilas Boas, J. M. A., & Martins, C. J. A. P. 2017, *Phys. Rev. D*, 96, 083012
- Maggiore, M., *Gravitational Waves* (Oxford University Press, 2007).
- Mandel, I., Sesana, A., & Vecchio, A. 2018, *Classical and Quantum Gravity*, 35, 054004
- Nakamura, T., Ando, M., Kinugawa, T., et al. 2016, *Progress of Theoretical and Experimental Physics*, 2016, 093E01
- Ni, W.-T., Wang, G., & Wu, A.-M. 2019, arXiv e-prints, arXiv:1909.04995
- Nomoto, K. 1982, *ApJ*, 253, 798
- Pakmor, R., Kromer, M., Röpke, F. K., et al. 2010, *Nature*, 463, 61
- Pakmor, R., Kromer, M., Taubenberger, S., et al. 2012, *ApJ*, 747, L10
- Ruiter, A. J., Belczynski, K., Benacquista, M., et al. 2010, *ApJ*, 717, 1006
- Saio, H., & Nomoto, K. 1985, *A&A*, 150, L21
- Sato, Y., Nakasato, N., Tanikawa, A., et al. 2015, *ApJ*, 807, 105
- Seto, N., Kawamura, S., & Nakamura, T. 2001, *Phys. Rev. Lett.*, 87, 221103
- Shen, K. J., & Bildsten, L. 2014, *ApJ*, 785, 61
- Shen, K. J., Kasen, D., Miles, B. J., et al. 2018, *ApJ*, 854, 52
- Sullivan, M., Le Borgne, D., Pritchett, C. J., et al. 2006, *ApJ*, 648, 868
- Totani, T., Morokuma, T., Oda, T., et al. 2008, *PASJ*, 60, 1327
- van den Broek, D., Nelemans, G., Dan, M., et al. 2012, *MNRAS*, 425, L24
- Webbink, R. F. 1984, *ApJ*, 277, 355
- Whelan, J., & Iben, I. 1973, *ApJ*, 186, 1007
- Willems, B., Kalogera, V., Vecchio, A., et al. 2007, *ApJ*, 665, L59
- Woosley, S. E., & Kasen, D. 2011, *ApJ*, 734, 38